

Article

Application of Genetic Algorithm for Inter-Turn Short Circuit Detection in Stator Winding of Induction Motor

Marcin Tomczyk ¹, Ryszard Mielnik ¹, Anna Plichta ², Iwona Gołdasz ³ and Maciej Sułowicz ^{1,*}

- ¹ Faculty of Electrical and Computer Engineering, Cracow University of Technology, Warszawska 24 Str., 31-155 Cracow, Poland; marcin.tomczyk@pk.edu.pl (M.T.); ryszard.mielnik@pk.edu.pl (R.M.)
- ² Faculty of Computer Science and Telecommunications, Cracow University of Technology, Warszawska 24 Str., 31-155 Cracow, Poland; anna.plichta@pk.edu.pl
- ³ Faculty of Environmental and Power Engineering, Cracow University of Technology, Warszawska 24 Str., 31-155 Cracow, Poland; iwona.goldasz@pk.edu.pl
- * Correspondence: maciej.sulowicz@pk.edu.pl

Abstract: This paper presents a new method of inter-turn short-circuit detection in cage induction motors. The method is based on experimental data recorded during load changes. Measured signals were analyzed using a genetic algorithm. This algorithm was next used in the diagnostics procedure. The correctness of fault detection was verified during experimental tests for various configurations of inter-turn short-circuits. The tests were run for several relevant diagnostic signals that contain symptoms of faults in an examined cage induction motor. The proposed algorithm of inter-turn short-circuit detection for various levels of winding damage and for various loads of the examined motor allows one to state the usefulness of this diagnostic method in normal industry conditions of motor exploitation.

Keywords: turn short circuit; stator winding; induction motor; genetic algorithm



Citation: Tomczyk, M.; Mielnik, R.; Plichta, A.; Gołdasz, I.; Sułowicz, M. Application of Genetic Algorithm for Inter-Turn Short Circuit Detection in Stator Winding of Induction Motor. *Energies* **2021**, *14*, 8523. <https://doi.org/10.3390/en14248523>

Academic Editor: Krzysztof Tomczyk

Received: 7 November 2021

Accepted: 11 December 2021

Published: 17 December 2021

Publisher's Note: MDPI stays neutral with regard to jurisdictional claims in published maps and institutional affiliations.



Copyright: © 2021 by the authors. Licensee MDPI, Basel, Switzerland. This article is an open access article distributed under the terms and conditions of the Creative Commons Attribution (CC BY) license (<https://creativecommons.org/licenses/by/4.0/>).

1. Introduction

Technical diagnostic is a process in which one checks the technical condition of an object and, from that, a decision is made about continuing to use it or subjecting it to a repair process enabling further use. In a special case, if the cost of repair is very high, the object is scrapped.

A system that allows one to detect, locate, and identify (classify) a fault is often simply called a fault detection system. Fast detection of a fault in its initial stage of formation prevents damage of components, unplanned breaks in the operation of the device, and life-threatening failure. An efficiently operating fault detection system limits possible economic losses caused by device malfunction. It uses generated signals that contain information about discrepancies between the nominal and incorrect working conditions of the device.

Mechanical, strongly nonlinear elements such as elastic-damper parts, bearing faults, or clearances occurring in elements have a strong influence on the operation of electromechanical systems in energy conversion. In such complex objects, analysis of diagnostics signals in the time-frequency domain and their classification is possible due to the application of transform methods. These methods allow for simultaneous investigation of spectra in both domains [1].

At the same time, there is constant progress in the field on new mathematical modeling methods that can be applied in diagnostics. Methods of modeling and identification elaborated based on automation with artificial intelligence techniques are currently being intensively developed in industry processes diagnostics [2].

In the past few years, there were published many papers presenting new fault detection techniques using time-frequency methods, neural networks, genetic algorithms, and image processing. It is worth noting some of them:

- Analysis of non-stationary vibration signal using Wigner–Ville time-frequency transform with Blackman’s time window [3],
- Bearing fault detection in cage induction motors using ST time-frequency analysis and acoustic signal autocorrelation function envelope analysis [4],
- Demonstration of the suitability of time-frequency analysis for inter-turn short-circuit detection in the stator winding of permanent magnet synchronous motor (PMSM) using improved wavelet analysis [5],
- Use of the discrete and packet wavelet transform for extracting particular features of the induction motor circuit currents for condition monitoring and failure mode detection [6],
- Innovative diagnostic method of inter-turn short circuit detection of linear start permanent magnet synchronous motor (LSPMSM) stator winding, using frequency analysis of acoustic signals with fast Fourier transform (FFT) [7],
- Use of stator load current analysis for various types of bearing fault of induction motor using fast Fourier transform and teaching convolutional neural network [8],
- Development of method of supply distortion (PQ) estimation for induction motors, based on the analysis of stator current with discrete wavelet transform coefficients, used both for one-directional feedforward neural network and neural network with radial function of neurons activation [9],
- Inertia of masses on motor shaft identification using wavelet transform of examined signals and neural network trained with error back propagation error method using Levenberg–Marquardt’s algorithm [10],
- Detection of rotor bar faults and stator winding short-circuit using Fourier transform and neural network [11],
- Diagnosis of induction motor using the model of neural network deep learning for automatic function training based on the data obtained from sensors and recognition of operating point [12],
- Presentation of possibilities of stator and rotor fault detection in induction motor using neural networks deep learning in analysis of axial flux variations [13],
- Analysis of bearing faults in induction motors using genetic algorithms and a combination of k nearest neighbors (KNN) algorithm, decision tree, and random forest (RF) [14],
- Application of a convolutional neural network for detecting and classifying winding faults in induction motor stators [15],
- Application of convergence and accuracy improvement of genetic algorithms in parametric identification of induction motor mathematical models [16],
- Demonstration of an identification method for parametric models of induction motors by means of a genetic algorithm [17],
- Presentation of a technique for detecting and localizing early-stage inter-turn faults in three-phase induction cage motors by means of genetic algorithms for estimating the motor nominal parameter values [18],
- Development of a differential evolution-based method for estimating electrical as well as mechanical parameter values of three-phase induction motors [19],
- Application of simulated annealing and evaporation rate water cycle algorithm (SA-ERWCA) for estimating parameter values of a reduced order model of an induction machine [20],
- Application of genetic algorithm in parameter identification of induction motor operating in a no-load state and without short-circuit tests [21],
- Development of an algorithm for optimal identification of induction motors by means of an evolutionary method—the so-called gravitational search algorithm (GSA) [22,23],
- Identification of fault in rotor winding using objective functions of genetic algorithms, which uses calculated errors of comparison of phase current signals for faulty and healthy induction motor models [24],

- Estimation of stator and rotor resistance, leakage reactance, and magnetizing reactance in an equivalent circuit of a three-phase induction motor using a combination of genetic algorithm and optimization of particle swarm (HGAPSO) [25],
- Combined approach based on artificial neural networks and genetic algorithms for calculating induction motor parameter values [26],
- Development of GA-based algorithms for an early-stage short-circuit related faults in stator windings of induction motors [27],
- Demonstration of a GA-CSA (crow search algorithm) hybrid algorithm for senseless control of induction motors [28],
- Efficient parameter estimation method for double-cage induction motors by means of the artificial bee colony (ABC) algorithm [29],
- Estimation of permanent magnet induction motor parameters for wheelchair applications by means of standard and dynamic particle swarm optimization algorithms (PSO), ant colony optimization (ACO), and artificial bee colony-based methods complemented by experimental methods [30],
- Presentation of method of cracked rotor bars detection in an induction motor using algorithm of processing of binary image developed from conversion of stator current vector [31],
- Introduction of a novel method for image clustering based on the classic Fuzzy C-Means (FCM) algorithm and the backtracking search algorithm (BSA) [32],
- Combination of three-phase inverter output currents image processing method and algorithm of nearest neighborhood (NN) for identification of faults occurring in induction motor drives [33], and
- Identification of inertia of masses on the shaft of induction motor drive by analyzing wavelet scalograms using the method of cauterization by k-means harmonics technique [34].

The rest of the paper is organized as follows: the second section contains a description of the laboratory stand and the examined induction motor with configurable stator winding. The principle of genetic algorithm operation is also described.

The third section contains a description of the results of the genetic algorithm application in inter-turn short-circuit identification based on the diagnostic signals obtained from laboratory measurements.

The fourth section contains conclusions on the application of the genetic algorithm in induction motor fault identification.

2. Laboratory Tests and Algorithm Description

Detecting winding short-circuit related faults at an early stage of failure is an important task in the maintenance and monitoring of electrical machines. To the best knowledge of the authors, this problem has not been fully researched and resolved to this day and is still an interesting research issue. Therefore, in order to develop a more effective algorithm for early detection of short-circuit faults, experimental tests were carried out, during which the data were obtained for the development of an efficient genetic algorithm.

2.1. Description of Research of Inter-Turn Short-Circuit Identification in Induction Motor Model

The subject of the research was an Sg-112M-4 cage induction motor with the following parameters: $P_n = 4.0$ kW, $U_n = 380$ V, $I_n = 8.6$ A, and $n_n = 1435$ rpm. The motor was mechanically coupled with a PZM5545 DC generator by a clutch. The DC generator works as a load for the induction motor and has the following parameters: $P_n = 4.5$ kW, $U_n = 230$ V, $I_n = 19.6$ A, $n_n = 1450$ rpm, and $I_f = 0.86$ A.

Figure 1 show the wiring diagram and terminals of stator coil turns. The number of the winding from which the turn is connected to the terminal on the board is marked with a number on the diagram by each turn.

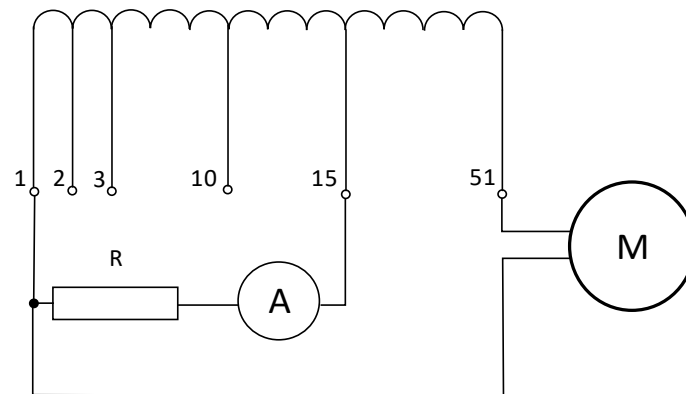


Figure 1. Wiring diagram of stator winding turns connection to the terminals.

Short circuit of selected winding was achieved by connecting the proper terminal of a turn with a resistor and ammeter, which was used for control of the current in shorted turns. Additional resistance of $5 \div 6 \Omega$ was used in order to protect the motor from overheating and to limit the current. The additional resistor does not have any impact on the results of the fault occurrence, which can be observed in investigated diagnostic signals.

Stator windings were connected in wye configuration and the motor was supplied from a three-phase low voltage network [35].

Apart from the modification of the induction motor winding, a coil for axial flux ϕ_1 measurement was mounted. The end shield of the examined motor is one of the most important parts of the laboratory stand for this experiment. The view of the end shield with installed measurement coil is presented in Figure 2.

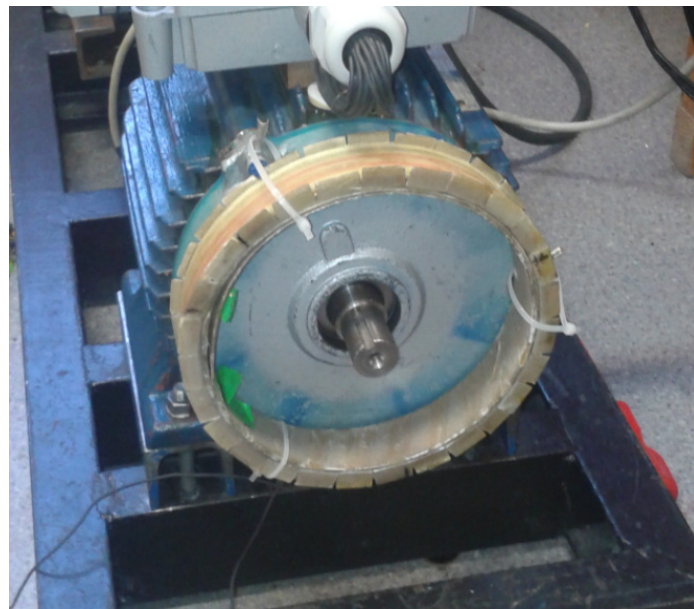


Figure 2. Stator of the examined motor with mounted coil for axial flux measurement.

The method of identifying inter-turn faults presented in the paper allows for an in-depth analysis of the results obtained from measurements. During the tests the registered parameter values were used, which were obtained from laboratory measurements of the induction motor behaviour and carried out on the laboratory stand described in this section.

It should be emphasized that the results here are obtained by means of an AI-based approach combining the GA algorithm and the discrete optimization method.

Analyzes were carried out in five groups of tests with the following five different values of load current I_{load} : 1A, 2A, 3A, 4A, and 5A. Each group of tests contained eight

different cases of inter-turn short-circuit. Tests results for all physical magnitudes and for each case of short-circuit change were put into matrix $X_{1[8,500000]}$. The elements of matrix X_1 were defined for each value of load current I_{load} . Formal changes were put into matrix K_1 in the following order: $K_1 = [(short\ circuit\ between\ turns\ 1\ and\ 2), (short\ circuit\ between\ turns\ 1\ and\ 3), (short\ circuit\ between\ turns\ 1\ and\ 4), (short\ circuit\ between\ turns\ 1\ and\ 5), (short\ circuit\ between\ turns\ 1\ and\ 10), (short\ circuit\ between\ turns\ 1\ and\ 15), (short\ circuit\ between\ turns\ 1\ and\ 20), (short\ circuit\ between\ turns\ 1\ and\ 25)]$.

In the proposed diagnostic method, analyses were carried out for the following physical magnitudes:

- (a) Turn short-circuit current I_z ,
- (b) Electromagnetic torque of the examined induction motor m_{el}
- (c) Voltage signal proportional to rotational speed of the rotor n_1 ,
- (d) Signal proportional to axial flux ϕ_1 ,
- (e) Vibration—acceleration in X axis— d_x ,
- (f) Vibration—acceleration in Y axis— d_y ,
- (g) Acoustic pressure— p_s ,
- (h) Phase voltages— $u_1, u_2,$ and u_3 ,
- (i) Phase currents— $i_1, i_2,$ and i_3 ,
- (j) Neutral point voltage— u_0 .

2.2. Description of Diagnostic Algorithm Applied in Processing of Examined Signals of Physical Magnitudes Using Genetic Algorithm of Simulated Annealing

In the diagnostic procedure assumed for all investigated physical magnitudes and performed for each examined case of inter-turn short-circuit there were used the values of matrix X_3 that were obtained by normalizing the elements of matrix X_1 and sorting the elements of matrix X_2 in descending order.

Analyses were performed with 50 kHz sampling frequency. The period of recorded signals of each test was 10 s.

Selected values of the matrix X_3 , which were used in calculations using genetic algorithm are defined as:

$$X_{3(i)(j)} = \begin{cases} [X_{2(i)(1)} \geq X_{2(i)(2)} \dots \geq X_{2(i)(300)}]; \\ i \in \langle 1, 8 \rangle; j = 1, 2, \dots, 300 \end{cases} \quad (1)$$

Normalization of X_1 elements' values was performed in identification experiments using:

- Parameters defined for acoustic pressure p_s for the first four assumed cases of inter-turn short circuit;
- Parameters defined for axial flux ϕ_1 for the last four assumed cases of inter-turn short circuit.

Identification tests were performed using the elements of reference matrices and elements of the examined matrix obtained from application of the genetic algorithm.

The values of the reference matrix were obtained from calculations of the genetic algorithm in which matrix X_2 was used for the group of tests for load current equal to $I_{load} = 3A$.

For all the examined physical magnitudes, the values of X_2 elements were calculated by narrowing the values of X_1 elements to the range $[a_3, a_4]$ as shown below:

$$X_{2((i)j)} = \begin{cases} \left(\frac{(X_{1(i)j} - a_{1(i)})}{(a_{2(i)} - a_{1(i)})} \right) * (a_{4(i)} - a_{3(i)}) + a_{3(i)}; \\ i \in \langle 1, 8 \rangle; j = 1, 2, \dots, 500000 \end{cases} \quad (2)$$

where:

X_1 —matrix elements values calculated during the test,

a_1 —minimum values of matrix X_1 elements defined in the test,
 a_2 —maximum values of matrix X_1 elements defined in the test,
 a_3 —initial value of the range containing normalized values of X_1 and calculated during the test of acoustic pressure p_s and during the test of axial flux,
 a_4 —end value of the range containing normalized values of X_1 and calculated during the test of acoustic pressure p_s and during the test of axial flux,
 i —number of examined inter-turn short-circuit case.

The values of variables $a_1, a_2, a_3,$ and a_4 were calculated using the following formulas:

$$a_{1(i)} = \min(X_{1(i)(j)}) \quad (3)$$

$$a_{2(i)} = \max(X_{1(i)(j)}) \quad (4)$$

$$a_{3(i)} = \begin{cases} \frac{\sum_{j=1}^{500000} X_{1(i)(j)}}{500000}; \\ X_{1(i)(j)} \text{ for } p_s, \phi_1 \end{cases} \quad (5)$$

$$a_{4(i)} = \begin{cases} \max(X_{1(i)(j)}); \\ X_{1(i)(j)} \text{ for } p_s, \phi_1 \end{cases} \quad (6)$$

Calculation of the values of examined matrix elements was performed by applying the genetic algorithm to elements of matrix X_2 calculated for a given load current I_{load} .

In the case of identification tests carried out using the values of the examined matrix, the following was applied:

- Calculation of matrix X_2 elements' values using Formula (2) and performed for the assumed first four cases of inter-turn short-circuit in which the normalization of matrix X_1 elements' values was done using parameters a_3 and a_4 calculated for acoustic pressure p_s ,
- calculations of matrix X_2 elements' values for assumed last four cases of inter-turn short-circuit in which the normalization of matrix X_1 elements' values was performed using additional operations using parameters calculated for axial flux ϕ_1 .

Calculations of X_1 matrix values performed by using additional operations with parameters defined from axial flux ϕ_1 were done for the case meeting the following condition:

$$a_{5(i)} \neq 0; i \in \langle 1, 8 \rangle \quad (7)$$

The value of variable a_5 is a maximum value defined by Chebyshev's distance for calculated elements' values of matrix X_6 according to the following formula:

$$a_{5(i)} = \max(X_{6(i)(1)}, X_{6(i)(2)}, X_{6(i)(3)}); i \in \langle 1, 8 \rangle \quad (8)$$

Values of X_6 matrix elements were obtained by calculating absolute values of differences between the values of elements of matrices X_4 and X_5 using the following formula:

$$X_{6(i)(j)} = |X_{4(i)(j)} - X_{5(i)(j)}|; i \in \langle 1, 8 \rangle; j = 1, 2, 3 \quad (9)$$

where:

X_4 —values of matrix elements calculated during the test,

X_5 —values of matrix X_4 elements calculated during the test for load current $I_{load} = 3A$.

Values of matrix X_4 elements were calculated by using the proper arithmetic mean values for the corresponding elements of X_3 matrix using the formulas shown below:

$$X_{4(i)} = [m_{1(i)}, m_{2(i)}, m_{3(i)}]; i \in \langle 1, 8 \rangle \quad (10)$$

$$m_{1(i)} = \frac{\sum_{j=1}^{100} X_{3(i)}}{100}; i \in \langle 1, 8 \rangle \quad (11)$$

$$m_{2(i)} = \frac{\sum_{j=101}^{200} X_{3(i)}}{100}; i \in \langle 1, 8 \rangle \quad (12)$$

where:

m_1, m_2, m_3 —arithmetic mean values of matrix X_3 elements calculated in the test.
The arithmetic mean values m_1, m_2 , and m_3 were calculated as follows:

$$m_{3(i)} = \frac{\sum_{j=201}^{300} X_{3(i)}}{100}; i \in \langle 1, 8 \rangle \quad (13)$$

The calculations of matrix X_2 values meeting the requirements defined by (7) were performed using the following formula:

$$X_{2((i)j)} = \begin{cases} \left(\frac{(X_{1(i)j} - a_{1(i)})}{(a_{2(i)} - a_{1(i)})} \right) * (a_{8(i)} - a_{7(i)}) + a_{7(i)}; \\ i \in \langle 1, 8 \rangle; j = 1, 2, \dots, 500000 \end{cases} \quad (14)$$

where:

a_7 —initial value of the range containing normalized values of X_1 and calculated during the test of axial flux ϕ_1 ,

a_8 —end value of the range containing normalized values of X_1 and calculated during the test of axial flux ϕ_1 .

The values of variables a_7 and a_8 were calculated using the following formulas:

$$a_{7(i)} = a_{9(i)} + \min(X_{1(i)j}); \quad i \in \langle 1, 8 \rangle \quad (15)$$

$$a_{8(i)} = \max(X_{1(i)j}) - a_{9(i)}; \quad i \in \langle 1, 8 \rangle \quad (16)$$

$$a_{9(i)} = \frac{\sum_{j=1}^{500000} X_{1(i)j}}{500000}; \quad i \in \langle 1, 8 \rangle \quad (17)$$

If the condition defined by (7) was not satisfied, calculations of matrix X_2 values are performed using Formula (2).

Parameters a_3, a_4, a_7 , and a_8 used in the calculations of matrix X_2 values were calculated for physical magnitudes such as acoustic pressure p_s and axial flux ϕ_1 . Application of these physical magnitudes was possible by satisfying the following conditions defined during tests for load current $I_{load} = 3A$:

$$a_{10} > a_{11}; \text{ for } i \in \langle 1, 4 \rangle \quad (18)$$

$$a_{12} > a_{13}; \text{ for } i \in \langle 5, 8 \rangle \quad (19)$$

where:

i —number of tested inter-turn short-circuit case.

Values of variables a_{10}, a_{11}, a_{12} , and a_{13} were calculated according to the following formulas:

$$a_{10} = \max(X_{7(i)}) - a_{11}; \quad i \in \langle 1, 4 \rangle \quad (20)$$

$$a_{11} = \left| \min(X_{7(i)}) \right|; \quad i \in \langle 1, 4 \rangle \quad (21)$$

$$a_{12} = \max(X_{7(i)}) - a_{13}; \quad i \in \langle 5, 8 \rangle \quad (22)$$

$$a_{13} = \left| \min(X_{7(i)}) \right| \quad i \in \langle 5, 8 \rangle \quad (23)$$

Values of matrix X_7 elements were calculated according to the following formulas:

$$X_{7(i)} = \max(X_{1(i)(j)}); \quad i \in \langle 1, 8 \rangle; j = 1, 2 \dots 500000 \quad (24)$$

For the proposed diagnostic method, one used the genetic algorithm of the highest growth. In the next iterations of this algorithm, for normalization of individual values, suitable values of the Fibonacci sequence were used. Values of matrix X_3 were used in calculations of Fibonacci sequence values stored in matrix X_8 .

Values of matrix X_8 elements are the values of five elements of the Fibonacci sequence and were calculated according to the formula shown below:

$$X_{8(i)(j)} = \begin{cases} X_{4(i)(j)}; & \text{for } j \leq 2 \\ X_{8(i)(j-1)} + X_{8(i)(j-2)}; & \text{for } j > 2 \\ i \in \langle 1, 8 \rangle; j = 1, 2 \dots 5 \end{cases} \quad (25)$$

where:

X_4 —values of X_4 elements calculated using Formula (10).

The Fibonacci sequence contains the proper values arranged in ascending order. This fact causes the increase in a wide range of the differences between the elements' values of the examined matrices obtained for different cases of inter-turn short-circuit. Hence the Fibonacci sequence can be effectively used in the identification process.

Definition of reference matrix elements' values used in the identification procedure of inter-turn short-circuit cases was the crucial step in presented diagnostic method.

Calculations in the described diagnostic procedure were performed according to genetic algorithm of the highest growth [36].

A block diagram showing the order of performing the calculations in the applied genetic algorithm of the highest growth is presented in Figure 3.

For the applied genetic algorithm, it was relevant to define an objective function. The choice of the objective function was made by using a series of simulation tests carried out for various objective functions. Based on the obtained results, Bohachevsky's function for the proper normalized individual values calculated for two arguments [36] was chosen as the objective function.

The calculations performed for individuals created in the population led to obtaining the first and second argument in the applied objective function.

Initialization of the population individuals is done in the initial stage of operation of the genetic algorithm of the highest growth.

The initial values of the individuals are random binary strings containing values of either 0 or 1.

Randomly selected binary strings in the population used for calculation of the first argument are stored in matrix X_9 , and binary strings in the population used for calculation of the second argument are stored in matrix X_{10} .

In the proposed diagnostic method, based on the results obtained for the series of simulation tests, it was assumed for the used genetic algorithm that the population size was 50 and the length of binary string for each population individual was equal to 20 or 25.

Processing of individuals' values in the presented genetic algorithm was stopped after satisfying the previously defined condition.

In the next iterations of the genetic algorithm realization, repeatable operations were performed.

In each iteration a binary string of the k th individual is selected, some amount of new different binary strings from the vicinity of the k th individual is chosen and the bits from these strings are replaced.

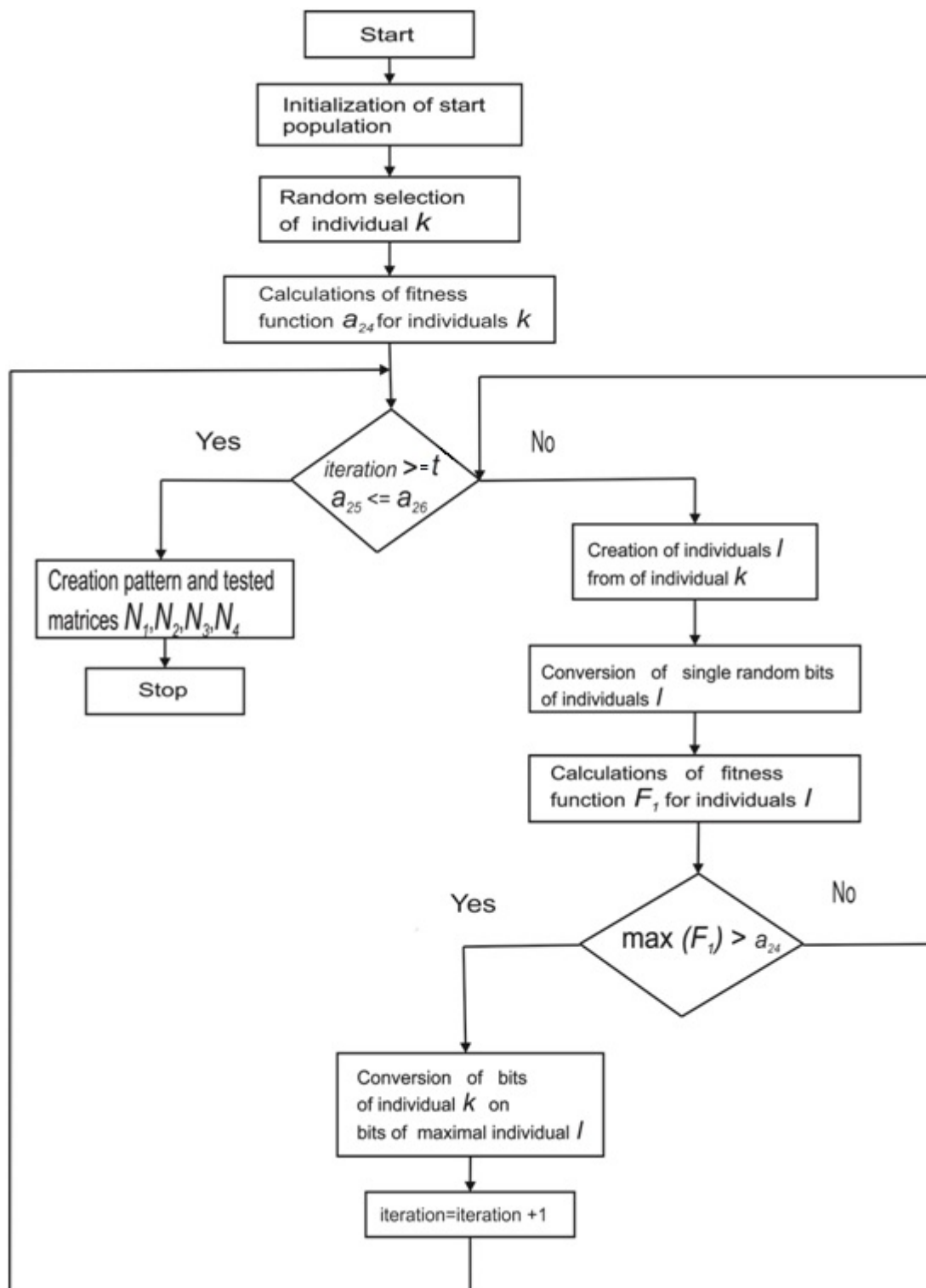


Figure 3. Block diagram of the genetic algorithm of the highest growth operation principle.

Selection of the k th individual from all the individuals in each population and replacement of the individual bits of some amount l of new individuals occurs in a random manner [36].

For such created binary strings in the vicinity of the k th individual, one chooses a string with the highest value of objective function.

If the highest value of the string from the vicinity of the k th individual is greater than the value of the objective function calculated for the binary string of the k th individual, then the proper exchange of the k th individual's binary string takes place [36].

In the presented genetic algorithm for all examined physical magnitudes, based on the observation of the results of a simulations series, a decision was made about using either 10 or 20 new different individuals.

In order to realize the described above steps of the genetic algorithm, the operations described below were performed.

In the first stage of the genetic algorithm, the binary string of k th individual was rewritten to new binary strings according to the formulas:

$$X_{11(l,j)} = \begin{cases} X_{9(k,j)}; \\ j = 1, 2 \dots m; k = \text{random}\langle 1, 50 \rangle; l = 1, 2 \dots n; \\ m \in \langle 20, 25 \rangle; n \in \langle 10, 25 \rangle \end{cases} \quad (26)$$

$$X_{12(l,j)} = \begin{cases} X_{10(k,j)}; \\ j = 1, 2 \dots m; k = \text{random}\langle 1, 50 \rangle; l = 1, 2 \dots n; \\ m \in \langle 20, 25 \rangle; n \in \langle 10, 25 \rangle \end{cases} \quad (27)$$

Next, replacement of individual bits of binary strings of various new l individuals occurs as follows:

$$X_{11(l,j)} = \begin{cases} 1 - X_{11(l,j)}; \\ j = \text{random} \langle 1, m \rangle; l = 1, 2 \dots n; \\ m \in \langle 20, 25 \rangle; n \in \langle 10, 25 \rangle \end{cases} \quad (28)$$

$$X_{12(l,j)} = \begin{cases} 1 - X_{12(l,j)}; \\ j = \text{random} \langle 1, m \rangle; l = 1, 2 \dots n; \\ m \in \langle 20, 25 \rangle; n \in \langle 10, 25 \rangle \end{cases} \quad (29)$$

The values of binary strings of one k th individual and new l individuals in the population were changed to decimal values using the formulas below:

$$a_{14(i)} = \sum_{j=1}^m X_{9(i)(k,j)} \cdot 2^{(j-1)}; i \in \langle 1, 8 \rangle; k = \text{random}\langle 1, 50 \rangle; m \in \langle 20, 25 \rangle \quad (30)$$

$$a_{15(i)} = \sum_{j=1}^m X_{10(i)(k,j)} \cdot 2^{(j-1)}; i \in \langle 1, 8 \rangle; k = \text{random}\langle 1, 50 \rangle; m \in \langle 20, 25 \rangle \quad (31)$$

$$X_{13(i)(l)} = \begin{cases} \sum_{j=1}^m X_{11(i)(l,j)} \cdot 2^{(j-1)}; \\ i \in \langle 1, 8 \rangle; l = 1, 2 \dots n; m \in \langle 20, 25 \rangle; n \in \langle 10, 25 \rangle \end{cases} \quad (32)$$

$$X_{14(i)(l,j)} = \begin{cases} \sum_{j=1}^m X_{12(i)(l,j)} \cdot 2^{(j-1)}; \\ i \in \langle 1, 8 \rangle; l = 1, 2 \dots n; m \in \langle 20, 25 \rangle; n \in \langle 10, 25 \rangle \end{cases} \quad (33)$$

where:

m —assumed length of binary string of a population individual.

Finding the most advantageous range of values' change for the suitable individuals in populations calculated using variables a_{14} and a_{15} and calculated matrices X_{13} and X_{14} according to the formulas given below was a very important step in this diagnostic procedure.

$$a_{22(i)} = \begin{cases} \left(\frac{(a_{14(i)} - a_{16(i)})}{(a_{17(i)} - a_{16(i)})} \right) * (a_{21(i)} - a_{20(i)}) + a_{20(i)}; \\ i \in \langle 1, 8 \rangle \end{cases} \quad (34)$$

$$a_{23(i)} = \begin{cases} \left(\frac{(a_{15(i)} - a_{18(i)})}{(a_{19(i)} - a_{18(i)})} \right) * (a_{21(i)} - a_{20(i)}) + a_{20(i)}; \\ i \in \langle 1, 8 \rangle \end{cases} \quad (35)$$

$$X_{15(i)(l,j)} = \begin{cases} \left(\frac{(X_{13(i)(l,j)} - a_{16(i)})}{(a_{17(i)} - a_{16(i)})} \right) * (a_{21(i)} - a_{20(i)}) + a_{20(i)}; \\ i \in \langle 1, 8 \rangle; j = 1, 2 \dots m; l = 1, 2 \dots n; \\ m \in \langle 20, 25 \rangle; n \in \langle 10, 25 \rangle \end{cases} \quad (36)$$

$$X_{16(i)(l,j)} = \begin{cases} \left(\frac{(X_{14(l)(l,j)} - a_{18(i)})}{(a_{19(i)} - a_{18(i)})} \right) * (a_{21(i)} - a_{20(i)}) + a_{20(i)}; \\ i \in \langle 1, 8 \rangle; j = 1, 2 \dots m; l = 1, 2 \dots n; \\ m \in \langle 20, 25 \rangle; n \in \langle 10, 25 \rangle \end{cases} \quad (37)$$

where:

a_{16} —minimum value of element a_{14} and elements of matrix X_{13} defined in the test,
 a_{17} —maximum value of element a_{14} and elements of matrix X_{13} defined in the test,
 a_{18} —minimum value of element a_{15} and elements of matrix X_{14} defined in the test,
 a_{19} —maximum value of element a_{15} and elements of matrix X_{14} defined in the test,
 a_{20} —initial value of the range containing normalized values of a_{14} , a_{15} , X_{13} , and X_{14} ,
defined in the test of matrix X_8 ,

a_{21} —end value of the range containing normalized values a_{14} , a_{15} , X_{13} , and X_{14} ,
defined in the test of matrix X_8 .

The values of the variables a_{16} , a_{17} , a_{18} , and a_{19} were defined using the following formulas:

$$a_{16(i)} = \begin{cases} \min(a_{14(i)}, X_{13(i)(l,j)}); \\ i \in \langle 1, 8 \rangle; j = 1, 2 \dots m; l = 1, 2 \dots n; \\ m \in \langle 20, 25 \rangle; n \in \langle 10, 25 \rangle \end{cases} \quad (38)$$

$$a_{17(i)} = \begin{cases} \max(a_{14(i)}, X_{13(i)(l,j)}); \\ i \in \langle 1, 8 \rangle; j = 1, 2 \dots m; l = 1, 2 \dots n; \\ m \in \langle 20, 25 \rangle; n \in \langle 10, 25 \rangle \end{cases} \quad (39)$$

$$a_{18(i)} = \begin{cases} \min(a_{15(i)}, X_{14(i)(l,j)}); \\ i \in \langle 1, 8 \rangle; j = 1, 2 \dots m; l = 1, 2 \dots n; \\ m \in \langle 20, 25 \rangle; n \in \langle 10, 25 \rangle \end{cases} \quad (40)$$

$$a_{19(i)} = \begin{cases} \max(a_{15(i)}, X_{14(i)(l,j)}); \\ i \in \langle 1, 8 \rangle; j = 1, 2 \dots m; l = 1, 2 \dots n; \\ m \in \langle 20, 25 \rangle; n \in \langle 10, 25 \rangle \end{cases} \quad (41)$$

The values of variables a_{20} and a_{21} were defined using the following formulas:

$$a_{20(i)} = \min(X_{8(i)(4)}, X_{8(i)(5)}); i \in \langle 1, 8 \rangle \quad (42)$$

$$a_{21(i)} = \max(X_{8(i)(4)}, X_{8(i)(5)}); i \in \langle 1, 8 \rangle \quad (43)$$

The values from the range $[a_{20}, a_{21}]$ of the variables a_{22} and a_{23} and the values of elements of matrices X_{15} and X_{16} were used in calculations of objective function.

The values of objective function a_{24} and F_1 were calculated using the formulas presented below:

$$a_{24(i)} = \begin{cases} a_{22(i)}^2 + 2 * a_{23(i)}^2 - 0.3 * \cos(3\pi * a_{22(i)}) - 0.4 * \cos(4\pi * a_{23(i)}) + 0.7; \\ i \in \langle 1, 8 \rangle \end{cases} \quad (44)$$

$$F_{1(i)(l)} = \begin{cases} X_{15(i)}^2 + 2 * X_{16(i)}^2 - 0.3 * \cos(3\pi * X_{15(i)}) - 0.4 * \cos(4\pi * X_{16(i)}) + 0.7; \\ i \in \langle 1, 8 \rangle; j = 1, 2 \dots m; l = 1, 2 \dots n; \\ m \in \langle 20, 25 \rangle; n \in \langle 10, 25 \rangle \end{cases} \quad (45)$$

where:

a_{24} —value of objective function of k th individual calculated in the test,

F_1 —value of objective function of l th individual calculated in the test.

Replacement of binary string of k th individual occurs in case of satisfying the following condition:

$$F_{1(i)(nr_1)} > a_{24(i)}; i \in \langle 1, 8 \rangle; nr_1 \in \langle 1, n \rangle; n \in \langle 10, 25 \rangle \quad (46)$$

where:

nr_1 —index of matrix F_1 containing the maximum value specified in the test.

Value of index nr_1 in matrix F_1 was defined by using the maximum value of this matrix:

$$F_{1(nr_1)} = \max(F_{1(l)}); i \in \langle 1, 8 \rangle; l = 1, 2 \dots n; n \in \langle 10, 25 \rangle \quad (47)$$

Binary string replacement of one k th individual was realized in the following manner:

$$X_{9(i)(k,j)} = \begin{cases} X_{11(i)(nr_1,j)}; \\ i \in \langle 1, 8 \rangle; j = 1, 2 \dots m; \\ k = \text{random}\langle 1, 50 \rangle; m \in \langle 20, 25 \rangle \end{cases} \quad (48)$$

$$X_{10(i)(k,j)} = \begin{cases} X_{12(i)(nr_1,j)}; \\ i \in \langle 1, 8 \rangle; j = 1, 2 \dots m; \\ k = \text{random}\langle 1, 50 \rangle; m \in \langle 20, 25 \rangle \end{cases} \quad (49)$$

It was assumed that the process of the applied genetic algorithm ends when the predefined amount of iterations is achieved and the following condition is satisfied:

$$a_{25(i)} \leq a_{26(i)}; i \in \langle 1, 8 \rangle \quad (50)$$

where:

a_{25} —value of the variable,

a_{26} —value of the variable.

In order to calculate the values of variables a_{25} and a_{26} , required calculations of l individuals' objective function maximum values obtained in five subsequent iterations of genetic algorithm were run. Calculations were run until the assumed number of iterations was reached.

The values of variables a_{25} and a_{26} were calculated using the formulas below:

$$a_{25(i)} = |a_{27(i)} - a_{28(i)}|; i \in \langle 1, 8 \rangle \quad (51)$$

$$a_{26(i)} = |m_{4(i)} - m_{5(i)}|; i \in \langle 1, 8 \rangle \quad (52)$$

where:

a_{27} —minimum value of elements of matrix X_{17} defined in the test, a_{28} —value of the median of elements of matrix X_{17} defined in the test, m_4 —arithmetic mean value of elements of matrix X_{17} calculated in the test,

m_5 —arithmetic mean value of elements of matrix X_{19} calculated in the test.

The values of variables a_{18} and a_{19} were defined according to the following formulas:

$$a_{27(i)} = \min(X_{17(i)(j)}); i \in \langle 1, 8 \rangle; j = 1, 2, \dots, 5 \quad (53)$$

$$a_{28(i)} = X_{18(i)(3)}; i \in \langle 1, 8 \rangle \quad (54)$$

The values of matrix X_{17} were defined using the values of matrix F_1 according to the formula:

$$X_{17(i)(j)} = \begin{cases} [F_{1(i)(nr_1)(t)}, F_{1(i)(nr_1)(t-1)} \dots F_{1(i)(nr_1)(t-4)}]; \\ i \in \langle 1, 8 \rangle; j = 1, 2, \dots, 5 \end{cases} \quad (55)$$

where:

t —iteration number of the applied genetic algorithm,

nr_1 —index of matrix F_1 containing the maximum value defined in the current iteration of the applied genetic algorithm according to the formula (47).

The values of matrix X_{18} were sorted as a result of sorting the matrix X_{17} in ascending order according to the formula:

$$X_{18(i)(j)} = \begin{cases} [X_{17(i)(1)} \leq X_{17(i)(2)} \dots \leq X_{17(i)(5)}]; \\ i \in \langle 1, 8 \rangle; j = 1, 2, \dots, 5 \end{cases} \quad (56)$$

Calculations of arithmetic means m_4 and m_5 were performed in the following manner:

$$m_{4(i)} = \frac{\sum_{j=1}^5 X_{17(i)(j)}}{5}; i \in \langle 1, 8 \rangle \quad (57)$$

$$m_{5(i)} = \frac{\sum_{j=1}^4 X_{19(i)(j)}}{4}; i \in \langle 1, 8 \rangle \quad (58)$$

All the values of matrix X_{17} excluding its maximum value were rewritten into a new matrix X_{19} . Performing such an operation improved the quality of obtained results from the inter-turn short-circuit identification process.

Elements of matrix X_{19} were obtained in the following manner:

$$X_{19(i)(j)} = X_{17(i)(j)}; i \in \langle 1, 8 \rangle; j = 1, 2, \dots, 4; j \neq nr_2 \quad (59)$$

where:

nr_2 —index of matrix X_{17} containing the maximum value defined in the test.

When the maximum value of the matrix X_{17} was defined, the index nr_2 was obtained:

$$X_{17(nr_2)} = \max(X_{17(j)}); i \in \langle 1, 8 \rangle; j = 1, 2, \dots, 5 \quad (60)$$

The cases of inter-turn short-circuit used in the tests with genetic algorithm were chosen according to some order defined in matrix K_1 .

Definition of reference matrices was made for eight assumed cases of inter-turn short-circuit for all investigated physical magnitudes.

The values of each reference matrix were calculated in test groups for which the load current was $I_{load} = 3A$, and they were saved into matrices of 8×3 dimensions: N_1 and N_2 .

The investigated values were saved into matrices of 1×3 dimensions: N_3 and N_4 .

After the genetic algorithm was finished, the values of matrix X_{18} were stored in matrices N_1 and N_2 containing reference values and in the tested matrices N_3 and N_4 . The matrices N_1 , N_2 , N_3 , and N_4 were defined according to the following formulas:

$$N_{1(i,j)} = X_{18(i,j)}; i = 1, 2, \dots, 8; j = 1, 2, \dots, 3 \quad (61)$$

$$N_{2(i,j)} = X_{18(i,j)}; i = 1, 2, \dots, 4; j = 1, 2, \dots, 3 \quad (62)$$

$$N_{3(j)} = X_{18(j)}; j = 1, 2, \dots, 3 \quad (63)$$

$$N_{4(j)} = X_{18(j)}; j = 1, 2, \dots, 3 \quad (64)$$

The results of identification tests were stored:

- in reference matrix N_1 and in examined matrix N_3 in case of normalization of matrix X_1 values performed using the parameters calculated for axial flux ϕ_1 ,
- in reference matrix N_2 and in examined matrix N_4 in case of normalization of matrix X_1 values performed using parameters calculated for acoustic pressure ps .

Calculation of the elements of matrices H_1 and H_2 allows for correct identification of inter-turn short-circuit case for calculated diagnostic signals of examined physical magnitudes at given load current I_{load} .

The values of matrices H_1 and H_2 were calculated using Euclidean metrics as shown below:

$$H_{1(i)} = \sum_{j=1}^3 \sqrt{(N_{1(i,j)} - N_{3(j)})^2}; i = 1, 2, \dots, 8 \quad (65)$$

$$H_{2(i)} = \sum_{j=1}^3 \sqrt{(N_{2(i,j)} - N_{4(j)})^2}; i = 1, 2, \dots, 4 \quad (66)$$

In the identification tests, the calculation of matrix H_1 values is performed in the first place.

After the index nr_3 in matrix H_1 is defined, matrix H_2 can be calculated. Such calculations are performed for the given index $nr_3 \in \langle 1, 4 \rangle$.

Obtained values of matrix H_1 ambiguously point to the correct number of examined cases of inter-turn short-circuits, hence the calculation of matrix H_2 is necessary.

Index nr_3 (for $nr_3 \in \langle 5, 8 \rangle$) in matrix H_1 points to a column in matrix K_1 that contains the right case of inter-turn short-circuit for the examined induction motor model.

Index nr_3 was defined by using the minimum value of matrix H_1 :

$$H_{1(nr_3)} = \min(H_{1(i)}); i \in \langle 5, 8 \rangle \quad (67)$$

The column number i of matrix K_1 refers to the corresponding index nr_3 ($i = nr_3$).

This leads to the conclusion that when index $nr_3 \in \langle 1, 4 \rangle$ is obtained, one gets index nr_4 in matrix H_2 . In this way it is possible for the tested induction motor model to correctly define the case of inter-turn short-circuits from the assumed first four cases. The column number in matrix K_1 refers to index nr_4 ($i = nr_4$).

Index nr_4 was calculated using the minimum value of matrix H_2 :

$$H_{2(nr_4)} = \min(H_{2(i)}); i = 1, 2, \dots, 4 \quad (68)$$

3. Results of the Diagnostic Algorithm Applied for Inter-Turn Short-Circuit Identification Occurring in Tested Induction Motor Model

Examined cases of inter-turn short-circuit used in genetic algorithm of the highest growth are presented in the tables below in a column called *Test Parameters*.

Moreover, the correct results from the identification process of inter-turn short-circuit cases, the results of matrices H_1 and H_2 calculations, are presented in the tables below and marked in bold.

The reference matrix N_1 was created for all investigated physical magnitudes in a given test group in which the load current I_{load} was equal to 3A.

Based on the obtained results one can state that obtaining the most suitable correct results of inter-turn short-circuit case identification for all examined physical magnitudes is possible when the diagnostic tests are carried out with the length of the binary string equal to the number l of new individuals, selected in populations from the vicinity of the k th individual.

It is worth noting that increasing the assumed number of iterations of the genetic algorithm and also the assumed length of the binary string of the individuals and the number of new individuals in the populations leads to obtaining visible differences in the results of fault identification. This conclusion results from the fact that the minimum values calculated in the H_1 and H_2 matrices were largely decreased.

The calculation results obtained in order to increase the values of the parameters noted above can be observed in all tables shown below.

To demonstrate the algorithm's efficiency as well as to highlight the quality of the results, Figure 4 illustrates the data registered during laboratory tests.

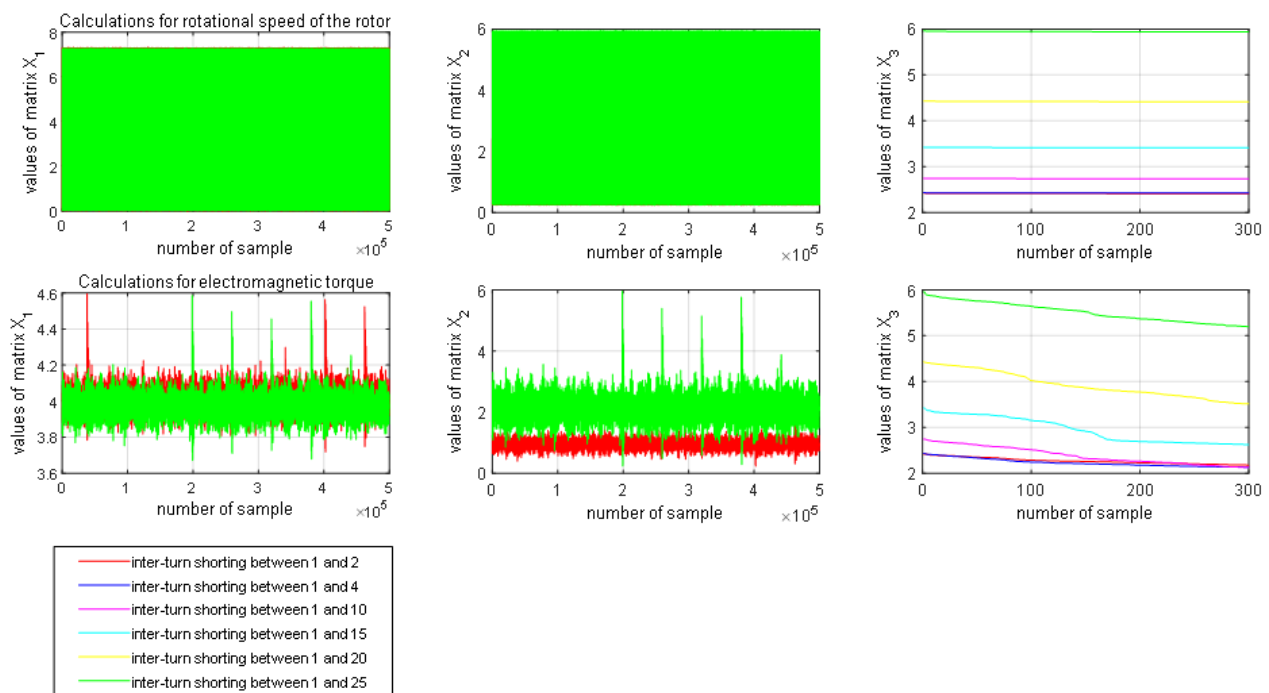


Figure 4. Presentation of the normalization of measurement data recorded in the X_1 matrix for the rotational speed n_1 and the electromagnetic moment m_{el} . The normalization was performed for the load current $I_{load} = 3A$ using the values of the variables a_3 and a_4 calculated for the axial flux ϕ_1 . The values of the X_2 matrix were sorted in descending order and stored in the X_3 matrix.

Tables 1–4 contain calculated coefficient values based on the data registered during the laboratory tests. The comparison reveals the efficiency of the modifications for the GA application.

Note that the compiled data in Tables 1–4 demonstrate the improvements in the efficiency of the proposed diagnostic method for early-stage inter-turn fault detection in induction motors. It is evident that incorporating the GA into the diagnostic procedure accelerates decision making.

Subsequent modifications of the algorithm and integrating it into online data acquisition systems and diagnostic systems will allow for the application of such methods in autonomous monitoring systems for arbitrary drive systems.

Table 1. Example results of matrix H_1 tests for electromagnetic torque m_{el} .

Test Parameters	Results* 10^3	Test Parameters	Results* 10^3
inter-turn short-circuit l_{10} , load current $I_{obc} = 1A$, population size = 50, binary string length = 20, number of individuals $l = 10$, assumed number of iterations = 50	0.0864 0.1023 0.0836 0.0833 0.0202 0.4030 1.0362 2.5904	inter-turn short-circuit l_{10} , load current $I_{obc} = 1A$, population size = 50, binary string length = 20, number of individuals $l = 20$, assumed number of iterations = 100	0.0843 0.0846 0.0756 0.0794 0.0083 0.4119 1.2553 2.7338
inter-turn short-circuit l_{15} , load current $I_{obc} = 5A$, population size = 50, binary string length = 25, number of individuals $l = 10$, assumed number of iterations = 50	0.5751 0.5712 0.5705 0.5579 0.4037 0.0865 0.7365 2.3907	inter-turn short-circuit l_{15} , load current $I_{obc} = 5A$, population size = 50, binary string length = 25, number of individuals $l = 25$, assumed number of iterations = 100	0.5418 0.5747 0.5322 0.5520 0.4838 0.0784 0.7694 2.1838

Table 2. Example results of matrix H_1 tests for rotational speed n_l .

Test Parameters	Results* 10^3	Test Parameters	Results* 10^3
inter-turn short-circuit l_{20} , load current $I_{obc} = 2A$, population size = 50, binary string length = 20, number of individuals $l = 10$, assumed number of iterations = 50	1.5636 1.5449 1.5455 1.5271 1.3159 0.8140 0.1065 1.6319	inter-turn short-circuit l_{20} , load current $I_{obc} = 2A$, population size = 50, binary string length = 20, number of individuals $l = 20$, assumed number of iterations = 100	1.5674 1.5549 1.5594 1.5280 1.3759 0.9142 0.0484 1.7621
inter-turn short-circuit l_{25} , load current $I_{obc} = 4A$, population size = 50, binary string length = 25, number of individuals $l = 10$, assumed number of iterations = 50	3.0284 3.0098 3.0141 2.9884 2.7960 2.2570 1.6319 0.6770	inter-turn short-circuit l_{25} , load current $I_{obc} = 4A$, population size = 50, binary string length = 25, number of individuals $l = 25$, assumed number of iterations = 100	3.0768 3.0190 3.0119 2.9865 2.8566 2.6018 1.7698 0.3653

Table 3. Example results of matrix H_2 tests for signal proportional to axial flux ϕ_1 .

Test Parameters	Results	Test Parameters	Results
inter-turn short-circuit 1_4, load current $I_{obc} = 2A$, population size = 50, binary string length = 20, number of individuals $l = 10$, assumed number of iterations = 50	7.3997 1.3367 0.9668 7.1590	inter-turn short-circuit 1_4, load current $I_{obc} = 2A$, population size = 50, binary string length = 20, number of individuals $l = 20$, assumed number of iterations = 100	7.5780 1.5661 1.1933 6.5498
inter-turn short-circuit 1_3, load current $I_{obc} = 4A$, population size = 50, binary string length = 25, number of individuals $l = 10$, assumed number of iterations = 50	5.4522 2.7054 9.3949 10.4065	inter-turn short-circuit 1_3, load current $I_{obc} = 4A$, population size = 50, binary string length = 25, number of individuals $l = 25$, assumed number of iterations = 100	5.8875 1.4312 8.1517 8.3732

Table 4. Example results of matrix H_2 tests for acceleration signal in X axis— d_x .

Test Parameters	Results	Test Parameters	Results
inter-turn short-circuit 1_2, load current $I_{obc} = 1A$, population size = 50, binary string length = 20, number of individuals $l = 10$, assumed iterations number = 50	0.1377 5.8630 11.0723 13.1808	inter-turn short-circuit 1_2, load current $I_{obc} = 1A$, population size = 50, binary string length = 20, number of individuals $l = 20$, assumed iterations number = 100	0.1130 5.8719 10.9845 13.5810
inter-turn short-circuit 1_5, load current $I_{obc} = 5A$, population size = 50, binary string length = 25, number of individuals $l = 10$, assumed number of iterations = 50	13.2778 7.1819 2.0972 1.0168	inter-turn short-circuit 1_5, load current $I_{obc} = 5A$, population size = 50, binary string length = 25, number of individuals $l = 25$, assumed number of iterations = 100	13.2797 7.4930 2.2323 0.9427

4. Conclusions

The presented fault detection system containing a diagnostic procedure based on a genetic algorithm allowing for calculation of the matrices resulting from the population individuals' values changes and objective function value changes can be applied in identification tests of various cases of inter-turn short circuit. The identification process was performed using the parameters varying in specified ranges defined for the samples of diagnostic signals. Application of the genetic algorithm significantly increases the effectiveness of non-stationary signals analysis.

This method used in diagnostic systems can effectively limit the after-effects of occurring faults because the effects of its application can be used in different stages of fault development.

In comparison with the clustering methods based on the standard Fuzzy C-Means (FCM) approach and the *backtracking search algorithm* (BSA) [32,37] as well as FOA type methods [38,39] or a multi-task optimization method combined with a hybrid differential evolution algorithm [40]. the presented inter-turn fault identification algorithm allows one to:

- Improve the results obtained for searching a locally optimal solution through clustering the data registered during the experiments and using the Bohachevsky objective function,
- Optimize the quality of the obtained data by varying parameters of the GA algorithm (the number of all individuals in the population and the number of new individuals l , the number of the binary chain/string and the assumed number of iterations and convergence condition),
- Apply it in continuous as well as discrete problem-solving tasks.

Advantages of the presented algorithm for the identification of internal faults involve obtaining the convergence of the genetic algorithm in terms of parameter changes, thus enabling the calculation of the optimal values used to identify the examined internal faults.

One disadvantage of the proposed detection method is the complex calculations of the GA convergence criterion.

Original or novel aspects of the proposed fault identification method for the examined induction motor model involve computing reference matrices for a selected group of tests and by means of the GA algorithm.

In addition to that, another novel aspect of the method is carrying out normalizing calculations by means of the obtained Fibonacci series values in subsequent iterations.

Based on the research, one can state that setting the right ranges of parameter change and narrowing the values of population individuals to suitable ranges leads to obtaining high effectiveness of fault detection and identification process.

Author Contributions: Conceptualization, M.T., R.M., A.P., I.G. and M.S.; methodology, M.T., A.P. and I.G.; software, M.T.; validation, R.M. and M.S.; formal analysis, M.T. and A.P.; investigation, R.M.; resources, M.S. and R.M.; data curation, M.T., R.M., A.P. and M.S.; writing—original draft preparation, M.T. and M.S.; writing—review and editing, M.T., R.M., I.G. and M.S.; visualization, A.P.; supervision, M.S. All authors have read and agreed to the published version of the manuscript.

Funding: This research was carried out under the theme Institute E-2 and was funded by the subsidies on science granted by the Polish Ministry of Science and Higher Education.

Institutional Review Board Statement: Not applicable.

Informed Consent Statement: Not applicable.

Data Availability Statement: Not applicable.

Conflicts of Interest: The authors declare no conflict of interest.

References

1. Kościelny, J.M.; Syfert, M.; Wnuk, P. Diagnostic Row Reasoning Method Based on Multiple-Valued Evaluation of Residuals and Elementary Symptoms Sequence. *Energies* **2021**, *14*, 2476. [[CrossRef](#)]
2. Calado, J.M.F.; Korbicz, J.; Patan, K.; Patton, R.J.; Sá da Costa, J.M.G. Soft computing approaches to fault diagnosis for dynamic systems. *Eur. J. Control* **2001**, *7*, 248–286. [[CrossRef](#)]
3. Duda, A.; Drozdowski, P. Induction Motor Fault Diagnosis Based on Zero-Sequence Current Analysis. *Energies* **2020**, *13*, 6528. [[CrossRef](#)]
4. Duda, A.; Sułowicz, M. A New Effective Method of Induction Machine Condition Assessment Based on Zero-Sequence Voltage (ZSV) Symptoms. *Energies* **2020**, *13*, 3544. [[CrossRef](#)]
5. Liang, H.; Chen, Y.; Liang, S.; Wang, C. Fault Detection of Stator Inter-Turn Short-Circuit in PMSM on Stator Current and Vibration Signal. *Appl. Sci.* **2018**, *8*, 1677. [[CrossRef](#)]
6. Khalid Abdulhassan, K.; Obed, A.; Hassan, S. Stator Faults Diagnosis and Protection in 3-Phase Induction Motor Based on Wavelet Theory. *J. Eng.* **2017**, *23*, 130–149.
7. Maraaba, L.S.; Twaha, S.; Memon, A.; Al-Hamouz, Z. Recognition of Stator Winding Inter-Turn Fault in Interior-Mount LSPMSM Using Acoustic Signals. *Symmetry* **2020**, *12*, 1370. [[CrossRef](#)]

8. Pandarakone, S.E.; Masuko, M.; Mizuno, Y.; Nakamura, H. Deep Neural Network Based Bearing Fault Diagnosis of Induction Motor Using Fast Fourier Transform Analysis. In Proceedings of the 2018 IEEE Energy Conversion Congress and Exposition (ECCE), Portland, OR, USA, 23–27 September 2018; pp. 3214–3221. [\[CrossRef\]](#)
9. Sridhar, S.; Rao, K.U.; Jade, S. Detection and Classification of Power Quality Disturbances in the Supply to Induction Motor using Wavelet Transform and Neural Networks. *Balk. J. Electr. Comput. Eng.* **2016**, *4*, 37–44.
10. Tomczyk, M.; Borowik, B.; Borowik, B. Identification of the mass inertia moment in an electromechanical system based on wavelet-neural method. *Appl. Comput. Sci.* **2018**, *4*, 96–111.
11. Ewert, P. Application of Neural Networks and Axial Flux for the Detection of Stator and Rotor Faults of an Induction Motor. *Power Electron. Drives* **2019**, *4*, 203–215. [\[CrossRef\]](#)
12. Shao, S.-Y.; Sun, W.-J.; Yan, R.; Wang, P.; Gao, R.X. A Deep Learning Approach for Fault Diagnosis of Induction Motors in Manufacturing. *Chin. J. Mech. Eng.* **2017**, *30*, 1347–1356. [\[CrossRef\]](#)
13. Skowron, M. Application of deep learning neural networks for the diagnosis of electrical damage to the induction motor using the axial flux. *Bull. Pol. Acad. Sci. Tech. Sci.* **2020**, *68*, 1031–1038. [\[CrossRef\]](#)
14. Toma, R.N.; Prosvirin, A.E.; Kim, J.-M. Bearing Fault Diagnosis of Induction Motors Using a Genetic Algorithm and Machine Learning Classifiers. *Sensors* **2020**, *20*, 1884. [\[CrossRef\]](#)
15. Skowron, M.; Orłowska-Kowalska, T.; Wolkiewicz, M.; Kowalski, C.T. Convolutional Neural Network-Based Stator Current Data-Driven Incipient Stator Fault Diagnosis of Inverter-Fed Induction Motor. *Energies* **2020**, *13*, 1475. [\[CrossRef\]](#)
16. Rutczyńska-Wdowiak, K. The scaling of fitness function in problem of parametric identification of induction motor mathematical model. *Przegląd Elektrotechniczny* **2017**, *R. 93, nr 10*, 149–153.
17. Rutczyńska-Wdowiak, K. The generating new individuals of the population in the parametric identification of the induction motor problem with the use of the genetic algorithm. *Czas. Tech.* **2019**, *2019*, 109–117. [\[CrossRef\]](#)
18. Aswad, R.A.K.; Jassim, B.M.H. Detection and Localization of the Stator Winding Inter-Turn Fault in Induction Motors based on Parameters Estimation using Genetic Algorithm. *J. Inst. Eng. India Ser. B* **2021**, 1–10. [\[CrossRef\]](#)
19. Guedes, J.J.; Castoldi, M.F.; Goedel, A.; Agulhari, C.M.; Sanches, D.S. Parameters estimation of three-phase induction motors using differential evolution. *Electr. Power Syst. Res.* **2018**, *154*, 204–212. [\[CrossRef\]](#)
20. Čalasan, M.; Micev, M.; Ali, Z.M.; Zobaa, A.F.; Aleem, S.H.E.A. Parameter Estimation of Induction Machine Single-Cage and Double-Cage Models Using a Hybrid Simulated Annealing–Evaporation Rate Water Cycle Algorithm. *Mathematics* **2020**, *8*, 1024. [\[CrossRef\]](#)
21. Postoyankova, K.; Polishchuk, V.; Shuvalova, A. Research of a Genetic Algorithm for Identification of Induction Motor Parameters. In Proceedings of the 2021 International Conference on Industrial Engineering, Applications and Manufacturing (ICIEAM), Sochi, Russia, 17–21 May 2021; pp. 334–338. [\[CrossRef\]](#)
22. Avalos, O.; Cuevas, E.; Gálvez, J. Induction Motor Parameter Identification Using a Gravitational Search Algorithm. *Computers* **2016**, *5*, 6. [\[CrossRef\]](#)
23. Cuevas, E.; Gálvez, J.; Avalos, O. Optimization Techniques in Parameters Setting for Induction Motor. *Stud. Comput. Intell.* **2019**, *854*, 9–25.
24. Aswad, R.A.K.; Jassim, B.M.H. Open-circuit fault diagnosis in three-phase induction motor using mode-based technique. *Arch. Electr. Eng.* **2020**, *69*, 815–827.
25. Mohammadi, H.R.; Akhavan, A. Parameter Estimation of Three-Phase Induction Motor Using Hybrid of Genetic Algorithm and Particle Swarm Optimization. *J. Eng.* **2014**, *2014*, 1–6. [\[CrossRef\]](#)
26. Tran, T.C.; Brandstetter, P.; Duy, V.H.; Dong, C.; Tran, C.D.; Ho, S.D. Estimate Parameters of Induction Motor Using ANN and GA Algorithm. In Proceedings of the AETA 2017—Recent Advances in Electrical Engineering and Related Sciences: Theory and Application. Thang University, Ho Chi Minh City, Vietnam, 7–9 December 2017; pp. 872–882. [\[CrossRef\]](#)
27. Duan, F.; Živanović, R. Induction Motor Stator Fault Detection by a Condition Monitoring Scheme Based on Parameter Estimation Algorithms. *Electr. Power Components Syst.* **2016**, *44*, 1138–1148. [\[CrossRef\]](#)
28. Tran, T.C.; Brandstetter, P.; Tran, C.D.; Ho, S.D.; Nguyen, M.C.H.; Phuong, P.N. Parameters Estimation for Sensorless Control of Induction Motor Drive Using Modify GA and CSA Algorithm. In Proceedings of the AETA 2018—Recent Advances in Electrical Engineering and Related Sciences: Theory and Application, Ostrava, Czech Republic, 11–13 September 2018; Springer: Cham, Switzerland, 2020; pp. 580–591. [\[CrossRef\]](#)
29. Jamadi, M.; Merrikh-Bayat, F. New Method for Accurate Parameter Estimation of Induction Motors Based on Artificial Bee Colony Algorithm. *arXiv* **2014**, arXiv:1402.4423.
30. Sankardoss, V.; Geethanjali, P. PMDC Motor Parameter Estimation Using Bio-Inspired Optimization Algorithms. *IEEE Access* **2017**, *5*, 11244–11254. [\[CrossRef\]](#)
31. Divdel, H.; Moghaddam, M.H.; Alipour, G. A new diagnosis of severity broken rotor bar fault based modeling and image processing system. *J. Curr. Res. Sci.* **2016**, *5*, 771–780.
32. Toz, G.; Yücedağ, İ.; Erdoğan, P. A fuzzy image clustering method based on an improved backtracking search optimization algorithm with an inertia weight parameter. *J. King Saud Univ.-Comput. Inf. Sci.* **2019**, *31*, 295–303. [\[CrossRef\]](#)
33. Bandyopadhyay, I.; Purkait, P.; Koley, C. A combined Image Processing and Nearest Neighbor Algorithm Tool for Classification of Incipient Faults in Induction Motor Drives. *Comput. Electr. Eng.* **2016**, *54*, 296–312. [\[CrossRef\]](#)

34. Tomczyk, M.; Plichta, A.; Mikulski, M. Application of image analysis to the identification of mass inertia momentum in electromechanical system with changeable backlash zone. *Appl. Comput. Sci.* **2019**, *15*, 87–102.
35. Zając, M.; Sułowicz, M. The detection of coil shorting in induction motors by means of wavelet analysis. *Tech. Trans.* **2016**, *Nr 2-E, Kraków*, 135–150.
36. Michalewicz, Z. *Genetic Algorithms + Data Structures = Evolution Programs*; Springer: Berlin/Heidelberg, Germany, 1996.
37. Wang, L.; Peng, L.; Wang, S.; Liu, S. Advanced backtracking search optimization algorithm for a new joint replenishment problem under trade credit with grouping constraint. *Appl. Soft Comput.* **2019**, *86*, 105953. [[CrossRef](#)]
38. Fan, Y.; Wang, P.; Mafarja, M.; Wang, M.; Zhao, X.; Chen, H. A bioinformatic variant fruit fly optimizer for tackling optimization problems. *Knowledge-Based Syst.* **2020**, *213*, 106704. [[CrossRef](#)]
39. Peng, L.; Zhu, Q.; Lv, S.-X.; Wang, L. Effective long short-term memory with fruit fly optimization algorithm for time series forecasting. *Soft Comput.* **2020**, *24*, 15059–15079. [[CrossRef](#)]
40. Sedak, M.; Rosić, B. Multi-Objective Optimization of Planetary Gearbox with Adaptive Hybrid Particle Swarm Differential Evolution Algorithm. *Appl. Sci.* **2021**, *11*, 1107. [[CrossRef](#)]